



Regular article

Self-similarity in the structure of coarsened nanoporous gold



Hansol Jeon^a, Na-Ri Kang^a, Eun-Ji Gwak^a, Jae-il Jang^b, Heung Nam Han^c, Jun Yeon Hwang^d, Sukbin Lee^{a,*}, Ju-Young Kim^{a,e,**}

^a School of Materials Science and Engineering, UNIST (Ulsan National Institute of Science and Technology), Ulsan 44919, Republic of Korea

^b Division of Materials Science and Engineering, Hanyang University, Seoul 04763, Republic of Korea

^c Department of Materials Science and Engineering, Seoul National University, Seoul 08826, Republic of Korea

^d Institute of Advanced Composite Materials, KIST (Korea Institute of Science and Technology), Jeonbuk 55324, Republic of Korea

^e KIST-UNIST Ulsan Center for Convergent Materials, UNIST, Ulsan 44919, Republic of Korea

ARTICLE INFO

Article history:

Received 12 April 2017

Received in revised form 7 May 2017

Accepted 7 May 2017

Available online xxxx

Keywords:

Annealing

3D reconstruction

Focused ion beam (FIB)

Cellular materials

Nanoporous gold

ABSTRACT

Nanoporous gold (np-Au) samples of ligament sizes 68.6, 248.6, 462.9, and 710.9 nm are prepared by heat treatment, and representative volumes are reconstructed by focused ion beam (FIB) tomography. The increase in relative density by thermal coarsening is not pronounced. We analyze the distribution of ligament size, surface-to-volume ratio, and scaled connectivity density for coarsened np-Au, revealing that np-Au coarsens in a self-similar way. The measured activation energy for thermal coarsening supports that it is accomplished by surface diffusion of Au.

© 2017 Published by Elsevier Ltd on behalf of Acta Materialia Inc.

Nanoporous gold (np-Au), which is composed of a bi-continuous network of Au ligaments and pores, has attracted attention in applications such as catalysis, sensors, and actuators [1,2]. Dealloying, selective dissolution of a less-noble elemental component from a precursor alloy, is an effective way to fabricate np-Au [3–5]. By post-heat treatment, the size of ligaments and pores can be coarsened up to microscales [6,7], and this feature size is critical in determining the mechanical and chemical properties of np-Au. In particular, the mechanical properties of np-Au are found to depend strongly on ligament size [6,8–10]; in general, the strength of np-Au increases as ligament size decreases, as in the size-dependent mechanical properties of nanopillars [11,12]. The Gibson-Ashby model [13], correlating mechanical properties and relative density of cellular materials, has been applied to describe np-Au's ligament-size-dependent mechanical behavior; however, there have been deviations due to various issues as well as high relative density of np-Au around 30% [10,14–18]. Modified scaling equations [10,19] have been suggested in the form of a function of relative density and ligament size based on experimental results. Sun et al. [20] investigated a variety of scaling laws in ligament-size-dependent mechanical properties by using molecular dynamics (MD) simulations. Liu et al. [21]

evaluated the network connectivity of np-Au using the concept of effective relative density by measuring elastic modulus. Understanding the irregular ligament structure in np-Au as well as its network connectivity is critical in mechanical behavior, and hence recently three-dimensional (3D) reconstruction experiments, tomography using transmission electron microscopy (TEM) [22,23], non-destructive X-ray tomography [24, 25], and serial cross-sectioning by focused ion beam (FIB) and reconstruction [26,27], have been applied. To study whether the ligament-size-dependent mechanical behavior of coarsened np-Au should be attributed to size-dependent material properties and/or to the evolution of nanoporous structure in terms of morphology and topology, it is very important to discover whether np-Au coarsens in a self-similar way or not. Although extensive computational and experimental work has given insight into this topic [25,27–31], the interpretation of self-similarity as np-Au coarsens is still under debate and the evidence still seems inconclusive.

We investigate the evolution of critical parameters in ligament-size-dependent mechanical behavior such as ligament size distribution, surface-to-volume ratio, and connectivity of coarsened np-Au. We prepare four coarsened np-Au samples with average ligament size 68.6, 248.6, 462.9, and 710.6 nm by free corrosion dealloying and post-heat treatment, and obtain reconstruction volumes using serial FIB cross-sectioning and scanning electron microscopy (SEM) imaging. The edge lengths of reconstruction volumes are set as 20–30 times the average ligament size to ensure that reconstruction volume contains enough ligaments

* Corresponding author.

** Correspondence to: J.-Y. Kim, School of Materials Science and Engineering, UNIST, Ulsan 44919, Republic of Korea.

E-mail addresses: sukbinlee@unist.ac.kr (S. Lee), juyoung@unist.ac.kr (J.-Y. Kim).

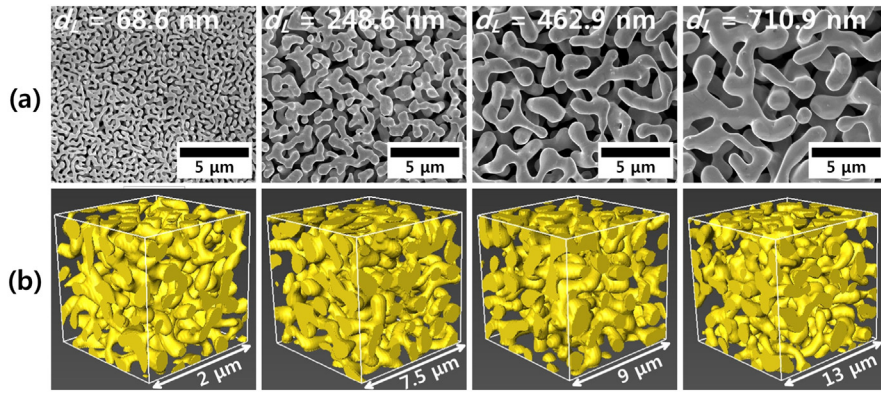


Fig. 1. (a) SEM images of coarsened np-Au samples and (b) volumes reconstructed by FIB-tomography.

to be representative, and >20 volumes are reconstructed for each sample for a statistical approach. Using experimental results, we discuss self-similarity of coarsened np-Au.

Pure Ag (99.99%) and Au (99.99%) pellets were melted to prepare Ag–Au precursor alloys (28 at.% Au–72 at.% Ag) at 1100 °C for 30 min, and homogenization was performed at 800 °C for 72 h under N₂ environment. Precursor alloys were cut into slices, one side of which was polished with 1 μm diamond suspension, and samples were annealed at 800 °C for 24 h. Dealloying by free corrosion was carried out in 35% nitric acid solution at 80 °C for 72 h. We obtained coarsened np-Au samples by heat treatment at 300 °C, 400 °C, 500 °C and 600 °C for 2 h. We measured neck diameters in connecting ligaments, possibly the thinnest part in connecting ligaments, using SEM (FE-SEM, FEI Nanolab 230); this is here called ‘average ligament size d_L ’. Amounts of residual Ag in at.% were measured by X-ray spectroscopy (EDX). Before 3D reconstruction, epoxy [KEM 90, ATM GmbH] was infiltrated into np-Au under high vacuum so that all pores were filled with solid epoxy, making it possible to obtain cleaner cross sections by FIB milling and to define clearly boundaries between ligaments and pores in two-dimensional (2D) images. 3D reconstructions were carried out using dual-beams system (FEI, Helios Nanolab 650). Cross-sectioning and taking SEM imaging were repeated automatically by an ‘auto slice and view’ program. The 200 cross-sectional SEM images were reconstructed in 3D by Avizo software [Avizo fire 8.1, FEI Visualization Sciences Group]. 3D reconstruction was accomplished by image filtering, segmentation, and mesh generation. Edge length of reconstructed volumes were set as 20–30 times of average ligament size. >20 volumes for each sample were reconstructed to alleviate stochastic uncertainty. The relative density of np-Au and surface-to-volume ratio were calculated using Avizo software. Connectivity and ligament size distribution were calculated using a BoneJ plug-in that is source of ImageJ [32].

Fig. 1 shows typical SEM and reconstructed 3D images of np-Au samples. Average ligament size d_L was measured as 68.6(±5.8) nm, 248.6(±24.9) nm, 462.9(±42.0) nm, and 710.6(±94.7) nm for np-Au heat-treated at 300 °C, 400 °C, 500 °C, and 600 °C, respectively. Fig. 2a shows the relation among the average ligament size d_L , the inverse ratio of ligament surface area to volume $1/S_V$, and the mean thickness $\langle D \rangle$. These parameters have been used to describe the characteristic ligament size of np-Au. The average ligament size d_L is the average diameter of necks in connecting ligaments, possibly the thinnest part measured by 2D SEM images. Although various measurement rules are possible, the average ligament size d_L can be intuitively understood in SEM images. $1/S_V$ and $\langle D \rangle$ can be calculated from parameters obtained during 3D reconstruction. S_V is the surface area per unit volume of the constituent solid, and $1/S_V$ has been suggested as a characteristic length scale of np-Au [26]. $\langle D \rangle$ is the average local thickness at any point that is the diameter of the largest sphere that contains this point and is inside the structure [33]. As shown in Fig. 2a, $1/S_V$ and $\langle D \rangle$ have very similar values for four samples, and these are also approximately proportional to d_L . Fig. 2b shows the relative density of np-Au calculated by reconstructed np-Au structures. Relative density increases gradually with increasing ligament size. However, the difference in relative density between $d_L = 68.6$ nm and $d_L = 710.6$ nm is only 1.8%, implying that any increase in relative density by sample shrinkage during thermal coarsening is not noticeable for these samples. Fig. 3a shows the distribution of local thickness normalized by the mean thickness $\langle D \rangle$. We obtained a probability density with integrated area 1 by fitting a Gaussian curve to histograms. Probability density curves for four samples almost overlap. This implies that even though ligaments in np-Au are randomly distributed for coarsened np-Au samples, distribution of ligament size normalized by mean thickness $\langle D \rangle$ is self-similar. Fig. 3b shows scaled S_V , $S_V \langle D \rangle$ as a function of average ligament size d_L . Surface-to-volume ratio S_V , also called as

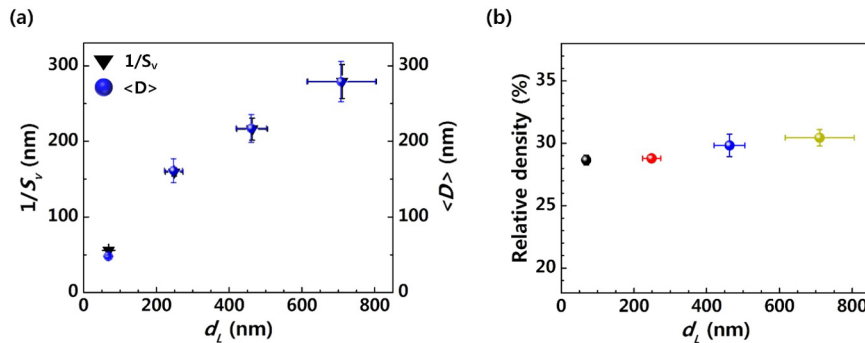


Fig. 2. (a) Comparisons of characteristic lengths of ligament size; average ligament size measured by SEM d_L , inverse of surface area-to-volume ratio $1/S_V$, and mean ligament thickness $\langle D \rangle$. (b) Relative density as a function of average ligament size.

specific surface area, can be used to estimate ligament morphology in nanoporous structures, which was suggested as a relevant parameter to characterize nanoporous structure [34]. Scaled S_V does not depend on ligament size, meaning that the surface area-to-volume ratio is self-similar for coarsened np-Au samples.

Connectivity is an important parameter in structural self-similarity of coarsened np-Au, since np-Au contains irregular load-bearing and dangling ligaments [16,17,21]. Fig. 3c shows that the scaled connectivity density, $C_V \langle D \rangle^3$ does not depend on ligament size. The connectivity C indicates the number of handles that can be cut before separating the structure into two pieces [35]; thus, the scaled connectivity density $C_V \langle D \rangle^3$ is the dimensionless connectivity density for establishing self-similarity of topological evolution. Euler characteristic χ was used to calculate connectivity, which in three dimension is given by [35,36]

$$\chi = n_0 - n_1 + n_2 - n_3, \quad (1)$$

where n_0 , n_1 , n_2 , and n_3 are the number of nodes, edges, faces, and voxels, respectively when each voxel has 26 neighbors. By using the Euler-Poincaré formula describing the relationship between connectivity and Betti numbers, and by taking into account that reconstructed volume consists of one interconnected solid with no isolated voids, the connectivity is given by

$$C = 1 - \Delta\chi, \quad (2)$$

where $\Delta\chi$ is the contribution of reconstructed volume to the Euler characteristic χ of the whole structure as calculated from reconstructed voxel parameters [35]. It should be noted that this is not a complete description of connectivity in terms of Minkowski functionals due to several issues such as intersection between slices and edge problems in the images. The results in Fig. 3c mean that density of connecting ligaments acting as load-bearing ligaments is similar for four coarsened np-Au samples and connectivity is self-similar for coarsened np-Au. The activation energy for coarsening Q is described by [25]

$$k \cdot t = \exp(-Q/RT), \quad (3)$$

where k is the characteristic ligament length; here the average ligament size d_L is used as this characteristic length; t is the heat-treatment time, R is the Boltzmann's constant, and T is the heat-treatment temperature. Heat-treatment at 300 °C, 400 °C, 500 °C and 600 °C for two hours yield an activation energy Q for coarsening of 34.1 kJ/mol, as shown in Fig. 4. This value is similar to that for surface diffusion in gold [37–39], and well below that for lattice diffusion in gold [40], indicating that thermal coarsening is carried out by surface diffusion. This finding is consistent with previous computational and experimental results [25,27,29]. Surface diffusion in np-Au during thermal coarsening can cause pinch-off of connecting ligaments and coalescence of torus ligaments, decreasing its connectivity [29,30]. Dead-end parts formed by pinch-off events have convex curvature, and tend to flatten to reduce surface energy, resulting in an increase in ligament size.

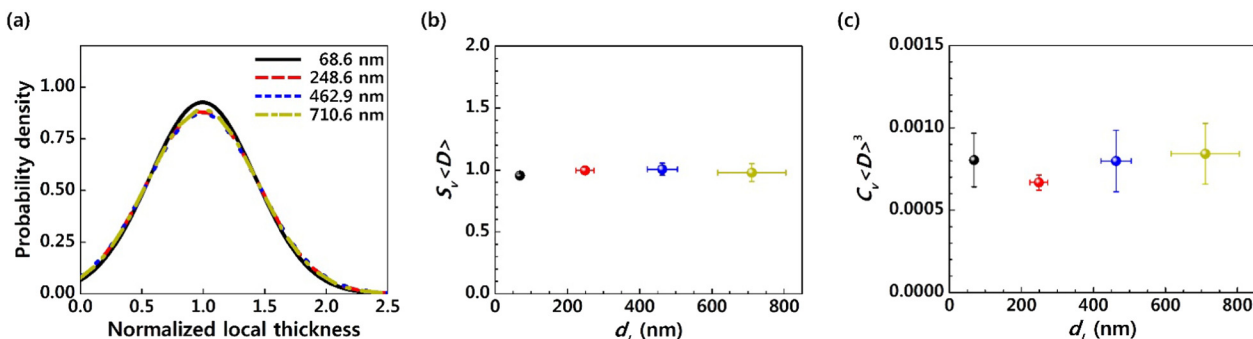


Fig. 3. (a) Distribution of mean ligament thickness, (b) scaled surface area-to-volume ratio, and (c) scaled connectivity density for coarsened np-Au.

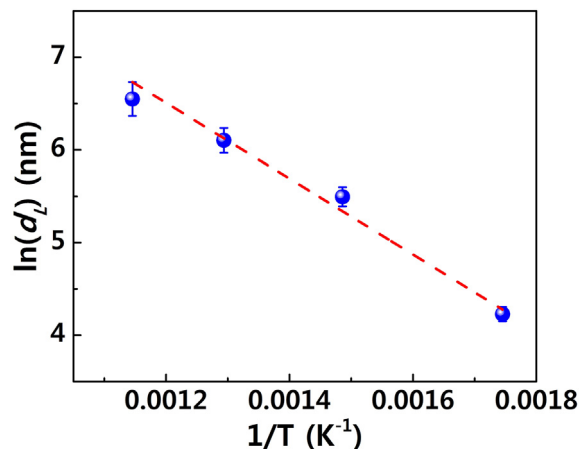


Fig. 4. Relation between average ligament size and heat-treatment temperature for calculation of activation energy for thermal coarsening in np-Au.

Np-Au has been reported to coarsen both in a self-similar and a non-self-similar way. Kertis et al. [7] found using SEM images that np-Au qualitatively appears to coarsen in a self-similar manner. Chen-Wiegart et al. [25], interpreting the the interfacial normal distribution (IND) and interfacial shape distribution (ISD) in np-Au reconstructed using X-ray tomography, suggested that the evolution of both surface orientation and scaled surface curvature is not self-similar during thermal coarsening. Liu et al. [21] showed that effective relative density increases gradually for ligament sizes greater than about 150 nm corresponding to an increase in connectivity with increasing ligament size; this is attributed to volume contraction and increase in relative density. Recently, Wang and Lilleodden [27,28], from FIB-tomography on coarsened np-Au, proposed that thermal coarsening occurs in a self-similar way in terms of the evolution of morphology with distribution of ligament size, scaled surface curvature, and evolution of topology with scaled connectivity density. As in this work, our results support the proposition that np-Au coarsens in a self-similar way by heat treatment in terms of distribution of ligament size, scaled surface-to-volume ratio, and scaled connectivity density.

Self-similarity in coarsened np-Au was investigated by 3D reconstruction using FIB-tomography for coarsened np-Au prepared by heat treatments at 300 °C, 400 °C, 500 °C, and 600 °C for two hours. We found that the increase in relative density by thermal coarsening is insignificant and that thermal coarsening is controlled by surface diffusion. The distribution of ligament size is self-similar, which is helpful in interpreting sequential deformation by statistical distribution of ligament size. Surface-to-volume ratios and scaled connectivity densities also indicate that np-Au coarsened in a self-similar way. These findings are critical in investigating mechanical properties of coarsened np-Au. Incipient plasticity and sequential deformation strongly depend on distribution of ligament size rather than characteristic ligament size.

Surface roughness of ligaments can be described by surface-to-volume ratio, which determines the stress concentration at ligament surface. Connectivity describes density of load-bearing ligaments that is directly related with strength and stiffness. This work should trigger work on the specifics of change in ligament shape and preferred orientation, and on the relationship of structural self-similarity and mechanical properties of np-Au.

This work was supported by the National Research Foundation of Korea (NRF) grant funded by the Ministry of Science, ICT & Future Planning (MSIP) (NRF-2015R1A5A1037627), by the KIST-UNIST partnership program (1.160097.01/2.160482.01), and by the Global Frontier R&D Program on Center for Multiscale Energy System funded by the National Research Foundation under the Ministry of Science, ICT & Future Planning, Korea (2012M3A6A7054855).

References

- [1] T. Fujita, P. Guan, K. McKenna, X. Lang, A. Hirata, L. Zhang, T. Tokunaga, S. Arai, Y. Yamamoto, N. Tanaka, Y. Ishikawa, N. Asao, Y. Yamamoto, J. Erlebacher, M. Chen, *Nat. Mater.* 11 (9) (2012) 775–780.
- [2] J. Biener, A. Wittstock, L.A. Zepeda-Ruiz, M.M. Biener, V. Zielasek, D. Kramer, R.N. Viswanath, J. Weissmuller, M. Baumer, A.V. Hamza, *Nat. Mater.* 8 (1) (2009) 47–51.
- [3] J. Erlebacher, M.J. Aziz, A. Karma, N. Dimitrov, K. Sieradzki, *Nature* 410 (6827) (2001) 450–453.
- [4] J. Weissmuller, R.C. Newman, H.J. Jin, A.M. Hodge, J.W. Kysar, *MRS Bull.* 34 (8) (2009) 577–586.
- [5] E. Detsi, M. van de Schootbrugge, S. Punzhin, P.R. Onck, J.T.M. De Hosson, *Scripta Mater.* 64 (4) (2011) 319–322.
- [6] R. Li, K. Sieradzki, *Phys. Rev. Lett.* 68 (8) (1992) 1168–1171.
- [7] F. Kertis, J. Snyder, L. Govada, S. Khurshid, N. Chayen, J. Erlebacher, *JOM* 62 (6) (2010) 50–56.
- [8] C.A. Volkert, E.T. Lilleodden, D. Kramer, J. Weissmuller, *Appl. Phys. Lett.* 89 (6) (2006).
- [9] J. Biener, A.M. Hodge, J.R. Hayes, C.A. Volkert, L.A. Zepeda-Ruiz, A.V. Hamza, F.F. Abraham, *Nano Lett.* 6 (10) (2006) 2379–2382.
- [10] A.M. Hodge, J. Biener, J.R. Hayes, P.M. Bythrow, C.A. Volkert, A.V. Hamza, *Acta Mater.* 55 (4) (2007) 1343–1349.
- [11] M.D. Uchic, D.M. Dimiduk, J.N. Florando, W.D. Nix, *Science* 305 (5686) (2004) 986–989.
- [12] J.Y. Kim, J.R. Greer, *Acta Mater.* 57 (17) (2009) 5245–5253.
- [13] L.J. Gibson, M.F. Ashby, *Cellular solids: structure and properties*, 2nd ed., Cambridge University Press, Cambridge; New York, 1997.
- [14] T.J. Balk, C. Eberl, Y. Sun, K.J. Hemker, D.S. Gianola, *JOM* 61 (12) (2009) 26–31.
- [15] H.J. Jin, L. Kurmanaeva, J. Schmauch, H. Rosner, Y. Ivanisenko, J. Weissmuller, *Acta Mater.* 57 (9) (2009) 2665–2672.
- [16] N. Mameka, K. Wang, J. Markmann, E.T. Lilleodden, J. Weissmuller, *Mater. Res. Lett.* 4 (1) (2016) 27–36.
- [17] S.S.R. Saane, K.R. Mangipudi, K.U. Loos, J.T.M. De Hosson, P.R. Onck, *J. Mech. Phys. Solids* 66 (2014) 1–15.
- [18] E.J. Gwak, J.Y. Kim, *Nano Lett.* 16 (4) (2016) 2497–2502.
- [19] N.J. Briot, T.J. Balk, *Philos. Mag.* 95 (27) (2015) 2955–2973.
- [20] X.Y. Sun, G.K. Xu, X.Y. Li, X.Q. Feng, H.J. Gao, *J. Appl. Phys.* 113 (2) (2013).
- [21] L.Z. Liu, X.L. Ye, H.J. Jin, *Acta Mater.* 118 (2016) 77–87.
- [22] H. Rosner, S. Parida, D. Kramer, C.A. Volkert, J. Weissmuller, *Adv. Eng. Mater.* 9 (7) (2007) 535–541.
- [23] T. Fujita, L.H. Qian, K. Inoke, J. Erlebacher, M.W. Chen, *Appl. Phys. Lett.* 92 (25) (2008).
- [24] Y.C.K. Chen, Y.S. Chu, J. Yi, I. McNulty, Q. Shen, P.W. Voorhees, D.C. Dunand, *Appl. Phys. Lett.* 96 (4) (2010).
- [25] Y.C.K. Chen-Wiegart, S. Wang, Y.S. Chu, W.J. Liu, I. McNulty, P.W. Voorhees, D.C. Dunand, *Acta Mater.* 60 (12) (2012) 4972–4981.
- [26] K.R. Mangipudi, V. Radisch, L. Holzer, C.A. Volkert, *Ultramicroscopy* 163 (2016) 38–47.
- [27] K.X. Hu, M. Ziehmer, K. Wang, E.T. Lilleodden, *Philos. Mag.* 96 (32–34) (2016) 3322–3335.
- [28] M. Ziehmer, K.X. Hu, K. Wang, E.T. Lilleodden, *Acta Mater.* 120 (2016) 24–31.
- [29] J. Erlebacher, *Phys. Rev. Lett.* 106 (22) (2011).
- [30] K. Kolluri, M.J. Demkowicz, *Acta Mater.* 59 (20) (2011) 7645–7653.
- [31] O. Zinchenko, H.A. De Raedt, E. Detsi, P.R. Onck, J.T.M. De Hosson, *Comput. Phys. Commun.* 184 (6) (2013) 1562–1569.
- [32] M. Doube, M.M. Klosowski, I. Arganda-Carreras, F.P. Cordeliers, R.P. Dougherty, J.S. Jackson, B. Schmid, J.R. Hutchinson, S.J. Shefelbine, *Bone* 47 (6) (2010) 1076–1079.
- [33] T. Hildebrand, P. Rueggsegger, *J. Microsc.* 185 (1997) 67–75.
- [34] E. Detsi, E. De Jong, A. Zinchenko, Z. Vukovic, I. Vukovic, S. Punzhin, K. Loos, G. ten Brinke, H.A. De Raedt, P.R. Onck, J.T.M. De Hosson, *Acta Mater.* 59 (20) (2011) 7488–7497.
- [35] A. Odgaard, H.J.G. Gundersen, *Bone* 14 (2) (1993) 173–182.
- [36] K. Michielsen, H. De Raedt, J.T.M. De Hosson, *Adv. Imag. Elect. Phys.* 125 (2002) 119–194.
- [37] M. Drechsler, J.J. Metois, J.C. Heyraud, *Surf. Sci.* 108 (3) (1981) 549–560.
- [38] H. Gobel, P. Vonblanckenhagen, *Surf. Sci.* 331 (1995) 885–890.
- [39] I. Beszedá, I.A. Szabo, E.G. Gontier-Moya, *Appl. Phys. A Mater. Sci. Process.* 78 (7) (2004) 1079–1084.
- [40] E.A. Brandes, G.B. Brook, C.J. Smithells, in: E.A. Brandes, G.B. Brook (Eds.), *Smithells Metals Reference Book*, 7th Butterworth-Heinemann, Oxford; Boston, 1998.